A NOVEL WORST-CASE ROBUST BEAMFORMER BASED ON INTERFERENCE-PLUS-NOISE COVARIANCE RECONSTRUCTION AND UNCERTAINTY LEVEL ESTIMATION

Yunmei Shi[1], *Lei Huang*[2], *Cheng Qian*[1], *Yonghua Wang*[1], *Weixin Xie*[2], *and H. C. So*[3]

[1]Department of Electronic and Information Engineering
Harbin Institute of Technology, Harbin, China
[2]College of Information Engineering, Shenzhen University, Shenzhen, China
[3]Department of Electronic Engineering
City University of Hong Kong, Hong Kong, China

ABSTRACT

A variant of adaptive worst-case (WC) beamformer is devised in this paper, which is robust against arbitrary unknown signal steering vector (SSV) mismatches. Compared with the conventional WC beamforming approach, the proposed method is further improved in terms of robustness by reconstructing the interference-plus-noise covariance matrix (INCM) and adaptively adjusting the uncertainty level of the SSV errors. In particular, the INCM is obtained by using the Capon spatial spectrum as the power distribution, and then the uncertainty level is estimated by maximizing the output power. Simulation results are included to illustrate the superiority of the proposed method.

***Index Terms*—** Worst-case, robust beamforming, signal steering vector mismatch, uncertainty level, Capon spatial spectrum.

1. INTRODUCTION

Adaptive beamforming has been widely used in radar, sonar, seismology and wireless communications [1]-[3]. The performance of adaptive beamformers (BFs) is known to depend essentially on the availability of signal-free training snapshots [4]. However, in many applications such as mobile communications, passive location and radio astronomy, the signal-free training snapshots are usually unavailable. This poses a big challenge because if the signal component is present in the training snapshots, the conventional adaptive BF will suffer severe performance degradation [5]. Furthermore, in practical applications, the signal steering vector (SSV) of the desired signal may be imprecise due to the existence of array imperfections, which cause serious signal cancellation problem. Therefore, robust adaptive beamforming has received much attention, and various robust techniques have been proposed in the literature [6]-[11].

There are several efficient approaches to the design of robust adaptive BFs, e.g., the diagonal loading of the sample covariance matrix (SCM) [12], worst-case (WC) SSV optimization [13] and WC signal-to-interference-plus-noise ratio (SINR) maximization algorithms [14]. As a matter of fact, these methods belong to the class of diagonal loading method. They are robust against SSV errors if the diagonal loading factor is properly selected. However, the choice of the optimal diagonal loading factor is not clear in practice. Moreover, the presence of the signal-of-interest (SOI) in the training snapshots causes a great performance degradation especially at high signal-to-noise ratio (SNR) conditions. Recently, the work to remove the effect of SOI has been conducted by Khabbazibasmenjet *et al*. [15], Mallipeddi *et al*. [16] and Gu *et al*. [17].

In this paper, inspired by the WC beamforming [13], we devise a new beamforming approach with a reconstructed interference-plus-noise covariance matrix (INCM) and an adaptively adjusted uncertainty level of the SSV errors, which is referred to as the reconstructed robust WC-BF (RR-WC-BF). In particular, with the knowledge of the presumed direction-of-arrival (DOA) of the SOI, the INCM is reconstructed by exploiting the spatial spectrum distribution of the incoming signals. With the so-obtained INCM, the uncertainty level of the SSV errors is estimated by maximizing the output power meanwhile adopting a quadratic constraint which is used to prevent the corrected SSV from converging to any interference.

The rest of the paper is organized as follows. In Section 2, we present the data model and review the WC-BF. In Section 3, the proposed RR-WC-BF is derived. In Section 4, numerical examples are provided to compare the performance of the proposed method with other robust beamforming algorithms. Finally, conclusions are drawn in Section 5.

The following notations are used throughout the paper. Matrices and vectors are represented by bold upper-case and bold lower-case characters, respectively. Superscripts $(\cdot)^T$, $(\cdot)^H$ and $(\cdot)^*$ stand for transpose, conjugate transpose and conjugate, respectively. The $\Re\{\cdot\}$ and $\Im\{\cdot\}$ denote the real and imaginary parts of a complex number, respectively. The $E\{\cdot\}$ stands for mathematical expectation. The $||\cdot||_2$ and $|\cdot|$ denote the Euclidean norm and absolute value, respectively. The $\boldsymbol{I}$ and $\mathbf{0}$ represent the identity and zero matrices, respectively. The $\mathcal{N}(\mu, \sigma)$ stands for the standard normal distribution with mean μ and standard deviation σ.

2. PROBLEM FORMULATION

2.1. Signal Model

Consider an array with M antennas receiving a far-field narrowband signal $s_0(k)$ with the DOA θ_s. The array measurements are modeled as

$$\boldsymbol{x}(k) = \boldsymbol{a}(\theta_s)s_0(k) + \boldsymbol{x}_i(k) + \boldsymbol{n}(k) \tag{1}$$

where $\boldsymbol{a}(\theta_s)$ is the SSV of the SOI, $\boldsymbol{x}_i(k)$ and $\boldsymbol{n}(k)$ are the statistically independent components of the interferences and noise, respectively. Here, we assume that both the interferences and noise are uncorrelated with the SOI.

The output of the BF with the weight vector $\boldsymbol{w} = [w_1, \ldots, w_M]^T$ is given by

$$y(k) = \boldsymbol{w}^H \mathbf{x}(k). \tag{2}$$

The weight vector can be obtained through maximizing the SINR [5]

$$\text{SINR} = \frac{\boldsymbol{w}^H \mathbf{R}_{\text{s}} \boldsymbol{w}}{\boldsymbol{w}^H \mathbf{R}_{\text{in}} \boldsymbol{w}} \tag{3}$$

where

$$\mathbf{R}_{\text{s}} = E\{\boldsymbol{a}(\theta_s)s_0(k)s_0^*(k)\boldsymbol{a}^H(\theta_s)\} = \sigma_s^2 \boldsymbol{a}(\theta_s)\boldsymbol{a}^H(\theta_s) \tag{4}$$

$$\mathbf{R}_{\text{in}} = E\{(\mathbf{x}_i(k) + \boldsymbol{n}(k))(\mathbf{x}_i(k) + \boldsymbol{n}(k))^H\} \tag{5}$$

are the $M \times M$ desired signal matrix and INCM, respectively, and σ_s^2 denotes the power of the SOI. The problem of maximizing (3) is mathematically equivalent to minimum variance distortionless response beamforming

$$\min \boldsymbol{w}^H \mathbf{R}_{\text{in}} \boldsymbol{w} \quad \text{s. t.} \quad \boldsymbol{w}^H \boldsymbol{a}(\theta_s) = 1. \tag{6}$$

It is well known [5] that the optimal weight vector for (6) is:

$$\boldsymbol{w}_{\text{opt}} = \frac{\mathbf{R}_{\text{in}}^{-1}\boldsymbol{a}(\theta_s)}{\boldsymbol{a}^H(\theta_s)\mathbf{R}_{\text{in}}^{-1}\boldsymbol{a}(\theta_s)}. \tag{7}$$

Indeed, the exact $\mathbf{R}_{\text{in}}$ is unavailable even in practical signal-free applications. In the following, the SCM

$$\hat{\mathbf{R}} = \frac{1}{N}\sum_{k=1}^{N} \mathbf{x}(k)\mathbf{x}^H(k) \tag{8}$$

is used instead of (5). Here, N is the number of training snapshots. As a result, we get the sample matrix inversion BF (SMI-BF)

$$\boldsymbol{w}_{\text{opt}} = \frac{\hat{\mathbf{R}}^{-1}\boldsymbol{a}(\theta_s)}{\boldsymbol{a}^H(\theta_s)\hat{\mathbf{R}}^{-1}\boldsymbol{a}(\theta_s)}. \tag{9}$$

When the signal component is present in the training snapshots, the use of the SCM (8) in lieu of the true INCM (5) degrades the performance of the SMI-BF significantly [4]. Another shortcoming of the SMI-BF is that it is sensitive to the mismatch between the presumed SSV $\boldsymbol{a}(\theta_s)$ and actual SSV $\tilde{\boldsymbol{a}}(\theta_s)$. To overcome these shortcomings, numerous robust approaches have been proposed [8]-[14].

2.2. Preliminaries

In this section, we review the most popular WC-BF [13] which is based on the assumption that the norm of the SSV error vector $\boldsymbol{e}$ is bounded by some known constant $\varepsilon > 0$, that is

$$||\boldsymbol{e}||_2 \leq \varepsilon. \tag{10}$$

Then, the set of the actual SSV is a sphere

$$\mathcal{A}\{\varepsilon\} = \{\tilde{\boldsymbol{a}}(\theta_s) | \tilde{\boldsymbol{a}}(\theta_s) = \boldsymbol{a}(\theta_s) + \boldsymbol{e},\ ||\boldsymbol{e}||_2 < \varepsilon\}. \tag{11}$$

The corresponding optimization problem is given by

$$\min_{\boldsymbol{w}} \boldsymbol{w}^H \hat{\mathbf{R}} \boldsymbol{w}$$
$$\text{s. t. } |\boldsymbol{w}^H(\boldsymbol{a}(\theta_s) + \boldsymbol{e})| \geq 1,\ \ (\boldsymbol{a}(\theta_s) + \boldsymbol{e}) \in \mathcal{A}\{\varepsilon\}. \tag{12}$$

According to [13], the semi-infinite nonconvex quadratically constrained problem (12) can be written as the following convex second-order cone (SOC) problem:

$$\min_{\boldsymbol{w}} \boldsymbol{w}^H \hat{\mathbf{R}} \boldsymbol{w}$$
$$\text{s. t. } \Re\{\boldsymbol{w}^H \boldsymbol{a}(\theta_s)\} - 1 \geq \varepsilon ||\boldsymbol{w}||_2$$
$$\Im\{\boldsymbol{w}^H \boldsymbol{a}(\theta_s)\} = 0. \tag{13}$$

As a result, it can be easily solved using convex optimization software, such as CVX [18]. However, the WC-BF has a severe performance degradation at high SNRs. This is because the desired signal component is present in the training snapshots. Another problem of the WC-BF is that it is unclear how to appropriately choose the uncertainty level ε for the SSV.

3. PROPOSED ALGORITHM

In this section, a variant of adaptive WC-BF is proposed. Firstly, a robust strategy is considered by reconstructing an estimate of the INCM $\tilde{\mathbf{R}}_{\text{in}}$, and then $\tilde{\mathbf{R}}_{\text{in}}$ is used instead of $\mathbf{R}_{\text{in}}$ in (5). Secondly, the choice of the uncertainty level ε is addressed. Moreover, an approximate estimate of ε is provided at the end of this section.

3.1. Reconstructed WC-BF

Assume there are P interferences. Then (5) can be written as $\mathbf{R}_{\text{in}} = \sum_{i=1}^{P} \sigma_i^2 \boldsymbol{a}(\theta_i)\boldsymbol{a}^H(\theta_i) + \sigma_n^2 \boldsymbol{I}$, where σ_i^2, $i = 1, 2, \ldots, P$, is the power of the interference coming from θ_i

and $\boldsymbol{a}(\theta_i)$ is the corresponding SSV, and σ_n^2 is the noise power. In practical applications, however, the powers of the interferences and noise, are unknown. In order to reconstruct the INCM, we need to know the spatial spectrum distribution in all directions. To this end, we use the Capon spatial spectrum estimator

$$\hat{\mathrm{P}}(\theta) = \frac{1}{\boldsymbol{a}^H(\theta)\hat{\mathbf{R}}^{-1}\boldsymbol{a}(\theta)} \tag{14}$$

where $\boldsymbol{a}(\theta)$ is the SSV associated with the DOA θ. According to [17], the INCM can be reconstructed as

$$\tilde{\mathbf{R}}_{\text{in}} = \int_{\bar{\Theta}} \frac{\boldsymbol{a}(\theta)\boldsymbol{a}^H(\theta)}{\boldsymbol{a}^H(\theta)\hat{\mathbf{R}}^{-1}\boldsymbol{a}(\theta)} d\theta \tag{15}$$

where $\bar{\Theta}$ is the complement sector of Θ and Θ is an angular sector where the SOI is located. Because $\tilde{\mathbf{R}}_{\text{in}}$ collects all information on interference and noise components in the out-of-sector $\bar{\Theta}$ and excludes the desired signal information in Θ, the effect of the desired signal can be removed.

3.2. Adjustment of Uncertainty Level ε

As is shown in [13], [19], the choice of the uncertainty level ε has a significant impact on the performance of the WC-BF. According to (10), ε is associated with the level of mismatch between $\tilde{\boldsymbol{a}}(\theta_s)$ and $\boldsymbol{a}(\theta_s)$. However, in practical applications, the actual SSV $\tilde{\boldsymbol{a}}(\theta_s)$ is usually difficult to obtain due to the complex propagation environment. As a consequence, our suggestion is to adaptively adjust ε with respect to the SSV error vector $\boldsymbol{e}$.

Substituting the Capon BF (9) and the reconstructed INCM $\tilde{\mathbf{R}}_{\text{in}}$ into the objective function (6), the output power can be represented as

$$\tilde{\mathrm{P}}(\theta) = \frac{1}{\boldsymbol{a}^H(\theta)\tilde{\mathbf{R}}_{\text{in}}^{-1}\boldsymbol{a}(\theta)}. \tag{16}$$

The $\tilde{\mathrm{P}}(\theta)$ is maximized when $\boldsymbol{a}(\theta)$ is equal to the actual SSV $\tilde{\boldsymbol{a}}(\theta_s)$. Consequently, the optimal SSV can be estimated by maximizing $\tilde{\mathrm{P}}(\theta)$, or by minimizing $\boldsymbol{a}^H(\theta)\tilde{\mathbf{R}}_{\text{in}}^{-1}\boldsymbol{a}(\theta)$. Note that the presumed SSV $\boldsymbol{a}(\theta_s)$ should be utilized to exclude the trivial solution $\boldsymbol{a}(\theta) = \mathbf{0}$. As a result, using $\boldsymbol{a}(\theta_s) + \boldsymbol{e}$ in lieu of $\boldsymbol{a}(\theta)$ yields the cost function

$$\min_{\boldsymbol{e}} \quad (\boldsymbol{a}(\theta_s) + \boldsymbol{e})^H \tilde{\mathbf{R}}_{\text{in}}^{-1} (\boldsymbol{a}(\theta_s) + \boldsymbol{e}). \tag{17}$$

In order to prevent the corrected steering vector $\boldsymbol{a}(\theta_s) + \boldsymbol{e}$ from converging to any interference located in $\bar{\Theta}$, an inequality constraint

$$(\boldsymbol{a}(\theta_s) + \boldsymbol{e})^H \tilde{\mathbf{R}}_{\text{in}} (\boldsymbol{a}(\theta_s) + \boldsymbol{e}) \leq \boldsymbol{a}^H(\theta_s)\tilde{\mathbf{R}}_{\text{in}}\boldsymbol{a}(\theta_s) \tag{18}$$

should be exploited. Note that any scaling of the SSV does not affect the output SINR [17]. The problem can be further simplified by setting $\boldsymbol{a}^H(\theta_s)\boldsymbol{e} = 0$. Therefore, the optimization problem is reformulated as

$$\begin{aligned} \min_{\boldsymbol{e}} \quad & (\boldsymbol{a}(\theta_s) + \boldsymbol{e})^H \tilde{\mathbf{R}}_{\text{in}}^{-1} (\boldsymbol{a}(\theta_s) + \boldsymbol{e}) \\ \text{s. t.} \quad & \boldsymbol{a}^H(\theta_s)\boldsymbol{e} = 0 \\ & (\boldsymbol{a}(\theta_s) + \boldsymbol{e})^H \tilde{\mathbf{R}}_{\text{in}} (\boldsymbol{a}(\theta_s) + \boldsymbol{e}) \leq \boldsymbol{a}^H(\theta_s)\tilde{\mathbf{R}}_{\text{in}}\boldsymbol{a}(\theta_s). \end{aligned} \tag{19}$$

Recalling that $||\boldsymbol{e}||_2 \leq \varepsilon$, we set

$$\tilde{\varepsilon} = ||\boldsymbol{e}||_2 \tag{20}$$

and use it instead of ε. Therefore, the design criterion of the proposed RR-WC-BF is

$$\begin{aligned} & \min_{\boldsymbol{w}} \boldsymbol{w}^H \tilde{\mathbf{R}}_{\text{in}} \boldsymbol{w} \\ & \text{s. t.} \ \Re\{\boldsymbol{w}^H \boldsymbol{a}(\theta_s)\} - 1 \geq \tilde{\varepsilon}||\boldsymbol{w}||_2 \\ & \quad \Im\{\boldsymbol{w}^H \boldsymbol{a}(\theta_s)\} = 0. \end{aligned} \tag{21}$$

Because $\tilde{\mathbf{R}}_{\text{in}}$ is a positve-definite matrix, the problem in (21) is a feasible SOC problem and can be easily solved using the CVX.

4. SIMULATION RESULTS

In this section, we present a number of numerical examples that illustrate the superiority of the proposed RR-WC-BF. For comparison, empirical results of the SMI-BF [20], LSMI-BF [12] and WC-BF [13] are included. A uniform linear array consisting of $M = 10$ sensors with interspacing of half wavelength is considered. Two interferences are assumed to have DOAs $30°$ and $50°$. The interference-to-noise ratio is 20 dB. The SOI is presumed to arrived from $\theta_s = 5°$ and the angular sector of the SOI is set to be $\Theta = [\theta_s - 5°, \theta_s + 5°]$. As a result, the corresponding out-of-sector is $\bar{\Theta} = [-90°, \theta_s - 5°) \cup (\theta_s + 5°, 90°]$. When comparing the performance of the adaptive beamforming algorithms in terms of number of snapshots, the SNR is fixed at 20 dB. In the comparison of SINR versus SNR, the number of snapshots is fixed at 30. Moreover, the background noise is assumed to be spatially and temporally white Gaussian process with zero-mean and covariance matrix $\boldsymbol{I}$. The diagonal loading factor is taken as 5 dB for the LSMI-BF and the uncertainty level ε is fixed at $0.3M$ for the WC-BF. For each scenario, 200 Monte-Carlo runs are performed.

4.1. Example 1

In the first example, we consider a scenario where the actual SSV is known exactly. From Fig. 1(a), we observe that there is a minor gap for these robust methods at low SNRs, but when the SNR is higher than 0 dB, the performance gap of these methods becomes remarkable. That is due to the fact that the presence of the SOI in the training snapshots can

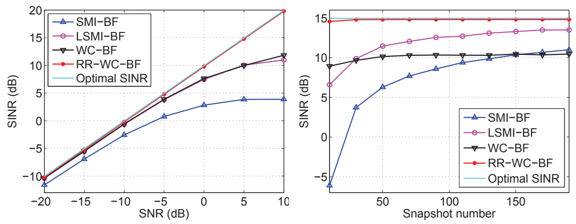

(a) (b)

Fig. 1. SINR of various BFs without SSV errors. (a) SINR versus SNR. (b) SINR versus snapshot number.

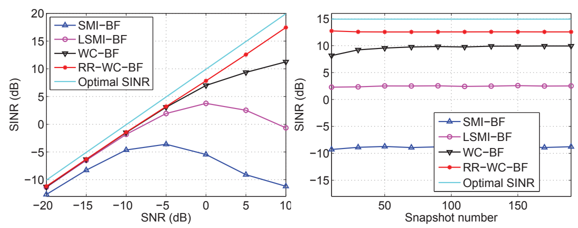

(a) (b)

Fig. 2. SINR of various BFs with 3° look direction mismatch. (a) SINR versus SNR. (b) SINR versus snapshot number.

cause a severe performance degradation at high SNRs. Moreover, the SINR of the proposed method is almost close to the optimal value. This in turn indicates that the proposed approach significantly outperforms the other algorithms.

4.2. Example 2

In this example, we assume that the actual DOA of the SOI is 8°, which corresponds to a 3° mismatch in the signal look direction. It is observed in Fig. 2 that although the performance of the RR-WC-BF is a little bit inferior to that of the first example, it still outperforms the other algorithms.

4.3. Example 3

In this example, the actual SSV is modeled as

$$\tilde{\boldsymbol{a}}(\tilde{\theta}_s) = [a_0 e^{j\pi \sin(\tilde{\theta}_s)}, \ldots, a_{M-1} e^{j\pi(M-1)\sin(\tilde{\theta}_s)}]^T \qquad (22)$$

where the array gains are denoted by $a_i = 1 + \bar{a}_i, i = 1, \ldots, M-1$, and $\bar{a}_i, i = 1, \ldots, M-1$, are independently drawn from $\mathcal{N}(0, 0.1)$, the DOA of the SOI is $\tilde{\theta}_s = \theta_s + \bar{\theta}_s$ and $\bar{\theta}_s$ is independently drawn from $\mathcal{N}(0, 2°)$. From Fig. 3, it is seen that the errors of the SSV have little influence on the performance of the proposed RR-WC-BF.

4.4. Example 4

In this example, we assume that the SOI is distorted by coherent local scattering effects. The actual SSV consists of

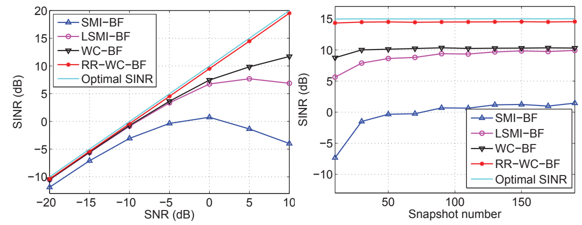

(a) (b)

Fig. 3. SINR of various BFs with random SSV errors. (a) SINR versus SNR. (b) SINR versus snapshot number.

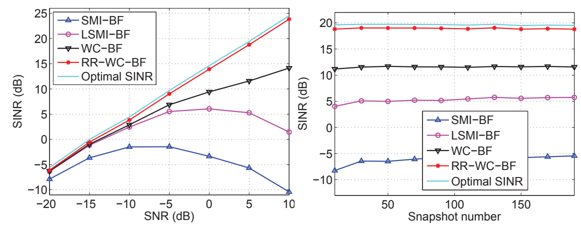

(a) (b)

Fig. 4. SINR of various BFs with incoherent local scattering. (a) SINR versus SNR. (b) SINR versus snapshot number.

five signal paths and is given by

$$\tilde{\boldsymbol{a}} = \boldsymbol{a}(\theta_s) + \sum_{i=1}^{4} e^{j\psi_i} \bar{\boldsymbol{a}}(\theta_i) \qquad (23)$$

where $\bar{\boldsymbol{a}}(\theta_i), i = 1, 2, 3, 4$, correspond to the coherently scattered paths. The DOAs $\theta_i, i = 1, 2, 3, 4$, are independently drawn from $\mathcal{N}(\theta_s, 4°)$ and $\psi_i, i = 1, 2, 3, 4$, are independently and uniformly distributed over $[0, 2\pi]$. Fig. 4 shows that the performance of the SMI-BF, LSMI-BF and WC-BF is still much worse than that of the RR-WC-BF especially at high SNRs.

5. CONCLUSION

In this paper, a new beamforming approach which is robust against arbitrary unknown SSV mismatches has been proposed. The robustness of the devised RR-WC-BF is enhanced by two strategies: INCM reconstruction and uncertainty level estimation. It is revealed that the INCM can be efficiently reconstructed with the knowledge of the presumed DOA of the SOI and the Capon spatial spectrum distribution. Meanwhile, based on the reconstructed INCM, the uncertainty level can be reliably estimated by maximizing the output power. Furthermore, the proposed RR-WC-BF is designed based on the WC-BF, which turns out to be robust against all kinds of array imperfections. Simulation results show that the output SINR of the proposed approach outperforms several conventional adaptive beamforming methods.

6. REFERENCES

[1] L. E. Brennan, J. D. Mallet and I. S. Reed, “Adaptive arrays in airborne MTI radar,” *IEEE Trans. Antennas Propagation*, vol. 24, no. 5, pp. 607-615, Sep. 1976.

[2] J. L. Krolik, “The performance of matched-field beamformers with Mediterranean vertical array data,” *IEEE Trans. Signal Process.*, vol. 44, no. 10, pp. 2605-2611, Oct. 1996.

[3] L. C. Godara, “Application of antenna arrays to mobile communications, part II: Beam-forming and direction-of-arrival considerations,” *Proc. IEEE*, vol. 85, no.8, pp. 1195-1245, Aug. 1997.

[4] D. D. Feldman and L. J. Griffiths, “A projection approach to robust adaptive beamforming,” *IEEE Trans. Signal Process.*, vol. 42, pp. 867-876, Apr. 1994.

[5] R. A. Monzingo and T. W. Miller, *Introduction to Adaptive Arrays.* New York: Wiley, 1980.

[6] H. L. Van Trees, *Detection, Estimation, and Modulation Theory, Part IV: Optimum Array Processing.* New York: Wiley, 2002.

[7] Z. L. Yu, Z . Gu, J . Zhou, Y . Li, S. Wee and M. H. Er, “A robust adaptive beamformer based on worst-case semi-definite programming,” *IEEE Trans. Signal Process.*, vol. 58, no. 11, pp. 5914-5919, 2010.

[8] S. A. Vorobyov, “Principles of minimum variance robust adaptive beamforming design,” *Signal Process.*, vol. 93, pp. 3264-3277, Nov. 2013.

[9] H. Ruan and R. C. de Lamare, “Robust adaptive beamforming using a low-complexity shrinkage-based mismatch estimation algorithm,” *IEEE Signal Process. Lett.*, vol. 21, no. 1, pp. 60-64, Jan. 2014.

[10] X. Jiang, W.-J. Zeng, A. Yasotharan, H. C. So and T. Kirubarajan, “Robust beamforming by linear programming,” *IEEE Trans. Signal Process.*, vol. 62, no. 7, pp. 1834-1849, Apr. 2014.

[11] X. Jiang, W.-J. Zeng, A. Yasotharan, H. C. So and T. Kirubarajan, “Minimum dispersion beamforming for non-Gaussian signals,” *IEEE Trans. Signal Process.*, vol. 62, no. 7, pp. 1879-1893, Apr. 2014.

[12] B. D. Carlon, “Covariance matrix estimation errors and diagonal loading in adaptive arrays,” *IEEE Trans. Aerosp. Electron. Syst.*, vol. 24, no. 4, pp. 397-401, Jul. 1988.

[13] S. A. Vorobyov, A. B. Gershman and Z. Q. Luo, “Robust adaptive beamforming using worst-case performance optimization: A solution to the signal mismatch problem,” *IEEE Trans. Signal Process.*, vol. 51, no. 2, pp. 313-324, Feb. 2003.

[14] S. J. Kim, A. Magnani, A. Mutapcic, S. P. Bovd and Z. Q. Luo, “Robust beamforming via worst-case SINR maximization,” *IEEE Trans. Signal Process.*, vol. 56, no. 4, pp. 1539-1547, Apr. 2008.

[15] A. Khabbazibasmenj, S. A. Vorobyov and A. Hassanien, “Robust adaptive beamforming via estimating steering vector based on semidefinite relaxation,” in *Proc. 44th Annu. Asilomar Conf. Signals, Systems, Computers*, Pacific Grove, CA, pp. 1102-1106, Nov. 2010.

[16] R. Mallipeddi, J. P. Lie, P. N. Suganthan, S. G. Razul and C. M. S. See, “Robust adaptive beamforming based on covariance matrix reconstruction for look direction mismatch,” *Progr. Electromagn. Res. Lett.*, vol. 25, pp. 37-46, Jul. 2011.

[17] Y. Gu and A. Leshem, “Robust adaptive beamforming based on interference covariance matrix reconstruction and steering vector estimation,” *IEEE Trans. Signal Process.*, vol. 60, no. 7, pp. 3881-3885, Jul. 2012.

[18] M. Grant, S. Boyd and Y. Y. Ye, CVX: MATLAB software for disciplined convex programming, Feb. 2007 [Online]. Avaliable: http:// www. stanford. edu/boyd/cvx/V.1.0RC3

[19] L. Landau, R. C. de Lamare and M. Haardt, “Robust adaptive beamforming algorithms based on the constrained constant modulus criterion,” *IET Signal Processing*, vol. 60, no. 7, pp. 3881-3885, Oct. 2013.

[20] I. S. Reed, J. D. Mallett and L. E. Brennan, “Rapid convergence rate in adaptive arrays,” *IEEE Trans. Aerosp. Electron. Syst.*, vol. AES-10, pp. 853-863, Nov. 1974.